

# Simulating the welding process of pin structures

Lukas Wittwer<sup>1</sup> and Norbert Enzinger<sup>1</sup>

<sup>1</sup> TU Graz, Institute for Material Science and Welding, Kopernikusgasse 24, 8010 Graz, Austria  
E-Mail: lukas.wittwer@tugraz.at

## ABSTRACT

Pin structures offer an innovative way of joining dissimilar materials such as metals and plastics based on an additional geometric link. Therefore pins are placed on a metal sheet substrate by use of a special arc welding technique called cold metal transfer (CMT), developed by Fronius International. The key element of the CMT process is a controlled back and forth movement of the wire during the welding process. This back and forth movement allows for welding pins.

In the context of pin welding, the welding process consists of three stages, warm up, cooling and shaping. During the warm up phase the welding wire is welded on the base material (stainless steel AISI 304). In the cooling stage the zone of maximum temperature is migrating within the wire to a certain position. When applying a current in the shaping phase the electric resistance is highest in the zone of maximum temperature, consequently the ohmic heating is strongest in this zone. In addition to the ohmic heating in a well-defined area the wire is pulled back mechanically causing the wire to rip off at certain distance from the joint. The height of the pins is in the millimeter range.

This work aims to describe the mechanical properties of a single pin based on its thermal history during the welding process. Thereby, we assume a given pin geometry derived from measurements of polished cross sections. In order to mimic the heat deposited in the welding process the Goldak heat source with optimized parameters is applied. Furthermore the occurring electric currents and voltages by means of an electro kinetic - thermal coupled analysis were taken into account.

## 1 Introduction

A very common and widely used method of joining metals and plastics is to use adhesives. Such joints can be improved by adding mechanical reinforcements such as bolts or rivets. The described techniques are well studied and are state of the art in many branches of industry like automotive or shipbuilding industry.

However, further developments in light weight design having increased the use of composite materials, e.g. carbon fiber reinforced plastics, demand for improvements in joining composites and metals. Pin structures on metal surfaces pose a mechanical reinforcement to ordinary adhesive joints with respect to forces perpendicular to the metal surface.

Furthermore, depending on the welding parameters three different kinds of shapes can be achieved, these are cylindrical, spiky and ball-headed pins. The shapes are depicted schematically in Figure 1.

In the case of fiber reinforced plastics the fibers may be woven around the pins or the pins can be impressed into the fiber mats and then be processed further. It has been demonstrated that

joints reinforced by pin structures exhibit a considerable increase of strength in comparison to joints without pins (see [1])

In this work we restricted ourselves to cylindrical pins made of stainless steel because the cylindrical geometry is easiest to handle in terms of finite element analysis. The filler material is stainless steel of the type AISI 308 and the base material is stainless steel AISI 304, Table 1 gives the composition of the used materials. These materials don't show metallurgical transitions during the welding process and are therefore appropriate for first basic calculations.

**Table 1: Chemical composition of the used materials. AISI 304 – plate, AISI 308 – pin**

	<b>C</b>	<b>Si</b>	<b>Mn</b>	<b>Cr</b>	<b>Ni</b>
<b>AISI 304</b>	≤ 0.05	0.5	1.4	18.5	9.5
<b>AISI 308</b>	≤ 0.02	0.8	1.7	20.0	10.2



**Figure 1: Schematic representation of differently shaped pins. The black bulk represents the base material and the light gray area is the attached part.**

The first part of this paper describes the used methods in detail. A description of the simulation process and the parameters for the thermal and mechanical analyses are provided.

In the second section the findings of some parameter studies are presented, further, results of temperature field calculations are given.

Finally, a short outlook on further investigations to be done concludes this work.

## 2 Process

As described before the welding process of a single pin is structured in several stages, those were adopted for finite element calculations yielding the following steps:

- **Stickout** During the stickout phase the wire tip is placed at the surface of the plate and a current of 100 A is applied for 2 ms causing to preheat the wire.
- **Heating** During this stage the arc burns in terms of FE analysis this means that the Goldak heat source is applied to the pin and the plate for 24 ms. Therefore, the Goldak source was split spatially in one part acting on the pin and another one acting on the plate. The thermal conductivity and heat capacity of the elements in between was set to  $10^{-6} \text{ Wmm}^{-1}\text{K}^{-1}$  and  $10^{-6} \text{ Jg}^{-1}\text{K}^{-1}$  respectively in order to prevent heat flow from the pin to the plate or vice versa. This assumption appears to be reasonable because during the real welding process, i.e. while the arc burns, wire and plate are separated from each other and thus any heat flow doesn't occur there. During this stage the thermal

expansion of the material is at the maximum. While the arc is burning the wire approaches the plate until it touches it, at this point the arc breaks down and the heating phase is done.

- **Pullback** After heating, the wire was pulled upwards for 3 ms. Furthermore, the thermal conductivity and heat capacity of the elements between pin and plate were set to values representing the proper material behavior at the acting temperature.
- **Calming** During this stage the whole system cools down, that is a phase when no thermal loads were applied to the system except for the boundary conditions. Due to the large volume of the plate compared to the wire most of the heat flows from the wire to the plate. As a consequence the zone of maximum temperature is migrating upwards in the wire.
- **Shaping** In this work we only consider cylindrically shaped pins. Therefore, after calming a current of 120 A was applied on the system and after a delay of 30 ms the preheated wire was pulled upwards. In order to model the shaping of the pin it is necessary to couple electro-kinetic thermal and mechanical calculations. Since SYSWELD does not provide such a tool we created a work around using a script written in SIL.

Figure 2a shows the mesh used for our calculations - Figure 2b in particular shows the region of the pin - plate interface. The thermal conductivity and the heat capacity of the elements marked 'interface' were set to  $10^{-6} \text{ Wmm}^{-1}\text{K}^{-1}$  and  $10^{-6} \text{ Jg}^{-1}\text{K}^{-1}$  while the heat source was active, i.e. pin and plate were thermally insulated.

The length of the wire corresponds to the weld parameter 'stickout' which is 12 mm, its diameter is 0.8 mm, and the thickness of the plate is 3 mm. The height of the pin socket as well as its horizontal expansion was derived from polished cross sections of real pins.

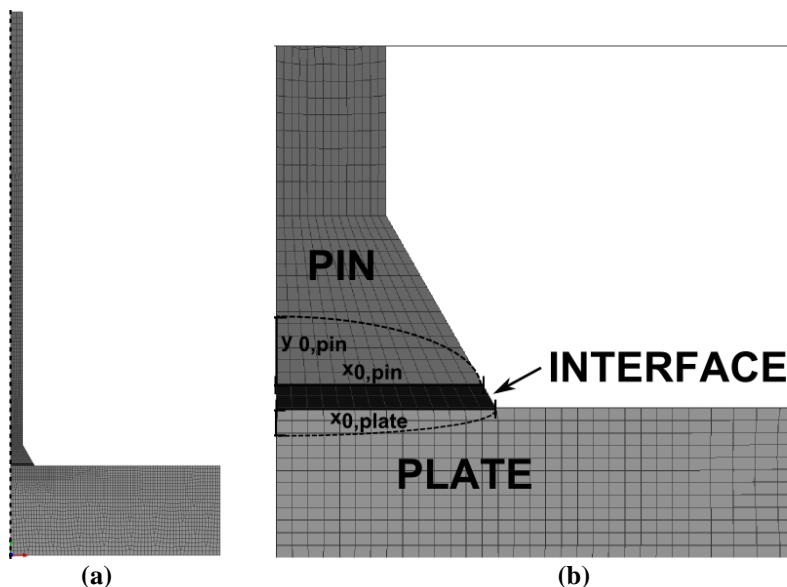


**Figure 2: Mesh of a plate and wire used in FE analysis. Picture (a) gives an overview over the whole mesh, the axis of symmetry is marked with a dotted line. In Figure (b) the interface of the pin and the plate are depicted. Further the parameters of the heat source are illustrated (compare Equation (1)).**

## 2.1 Thermal calculations

In order to mimic the heat input during the welding process of a pin, we used several models for the heat input in our calculations. Due to a single pin's axial symmetry the simulation can be limited to the positive x-y plane with the y-axis being the rotation axis.

At this point it should be mentioned that, since we were only performing thermal calculations, we used a predefined pin geometry, which is possible due to the high reproducibility of the process. This geometry was determined from polished cross sections. The thermo physical material parameters were taken from the SYSWELD database if not mentioned explicitly. An overview of the used parameters at room temperature is given in Table 2.

**Table 2: Thermal properties of stainless steel AISI 304 (plate) and AISI 308 (pin) at room temperature (20°C). Values with an asterisk were taken from the SYSWELD database.**

$\lambda$  ... thermal conductivity ( AISI 304 from SYSWELD database, AISI 308 from ASM Handbook)  
 $\rho^*$  ... Density  
 $c_p^*$  ... heat capacity

	$\lambda$ [Wmm <sup>-1</sup> K <sup>-1</sup> ]	$\rho$ [gmm <sup>-3</sup> ]	$c_p$ [Jg <sup>-1</sup> K <sup>-1</sup> ]
AISI 304	0.0162	7.9*10 <sup>-6</sup>	514
AISI 308	0.0139	7.9*10 <sup>-6</sup>	514

The three dimensional Goldak heat source (see [2]) turned out to be the best way to model the heat input for this welding process. In our radial-symmetric geometry the heat input due to Goldak reads as follows,

$$q = q_0 e^{-3\left(\frac{x}{x_0}\right)^2} e^{-3\left(\frac{y}{y_0}\right)^2} \quad (1)$$

$$q_0 = \eta \frac{6\sqrt{3}UI}{x_0^2 y_0 \sqrt{\pi\pi}} f \quad (2)$$

with  $x_0$  and  $y_0$  representing the width and the depth of the weld pool, respectively. The parameters U and I are the voltage and electric current defining in connection with the efficiency  $\eta$  the power input.

As mentioned above, the heat source was split into two parts, one acting on the plate and the other acting on the pin. The parameter f in Equation (1) describes how much power is deposited on the pin and the plate, respectively. Thus the value of f ranges from 0 to 1 in the pin and the plate and the sum of  $f_{pin}$  and  $f_{plate}$  must be equal to one due to energy conservation:

$$f = f_{pin} + f_{plate} = 1. \quad (3)$$

### 2.1.1 Boundary conditions

The boundary conditions describe the loss of energy due to radiation and convection at the edge of the work piece. The heat exchange of the work piece and the surrounding environment was

described by the 'lumped capacitance model' [3]. In this model the heat transfer coefficient for radiation reads as follows

$$h_{rad} = \sigma \varepsilon (T + T_0)(T^2 + T_0^2) \quad (4)$$

where  $T_0$  is the temperature of the surrounding medium. The quantity  $\sigma$  denotes the Boltzmann's constant and  $\varepsilon$  is the emissivity. In our case the surrounding medium was air with a temperature of 20°C and the emissivity was set to a value of 0.8 (compare [4]).

Heat loss due to convection was taken into account by an additional parameter  $h_c$  being the convective heat transfer coefficient. In contrast to radiation  $h_c$  was assumed to be constant in temperature.

Thus, the overall heat exchange of the work piece with its environment is described by the sum of radiation and convection:

$$h = h_{rad} + h_c \quad (5)$$

In case of convection the boundary of the system was divided in two sections of different convective heat transfer coefficients.

In the region of the interface of pin and plate the convective heat transfer coefficient was assumed to be higher than at the rest of the surface. This assumption appears to be reasonable since the loss of energy in this region is enhanced due to vortices of the shielding gas in this area.

The value for the convective heat transfer coefficient at the residual boundaries was set to 80  $\text{Wm}^{-2}\text{K}^{-1}$  as suggested in [4], for the interface region several calculations with different values for  $h_c$  were performed. In those calculations  $h_c$  in the pin socket region was multiplied by a factor  $k$  ranging from  $k = [1, 2.5]$ . However, the range of values for  $h_c$  at the interface was chosen for investigating its influence on the overall result. In order to get physical reasonable values fluid mechanical calculations are still to be performed.

The temperature at the nodes located on the lower side of the plate as well as those at the very top of the wire was constrained to 20 °C. These rigid boundary conditions take into account that those are not real surfaces exposed to the surrounding air. In the case of the top nodes, there is continuing wire and the bottom of the plate is in direct contact to the work bench.

## 2.2 Mechanical calculations

For the mechanical analysis we assumed plasticity with isotropic strain hardening. The respective temperature dependent material parameters were taken from the SYSWELD material database.

During the *pullback* phase the velocity in  $y$  direction for the top nodes of the wire was set to  $5\text{mms}^{-1}$ . Several nodes at the surface of the plate were restricted from moving in order to mimic the clamping of the work piece.

In the *shaping* stage the clamped nodes at the surface were fixed and the velocity of the nodes at the top was set to  $33\text{mms}^{-1}$ . The velocities applied during pullback and shaping were predefined from the welding program.

During the *shaping* process interactions between mechanics and thermo-electric effects must be considered. On the one hand the electrical resistance increases at the point of maximum temperature causing the wire to heat up further. Further, the contractions in the zone of elevated temperature lead to a reduced cross section and therefor to a rising electrical resistance.

In order to mimic the shaping process described above, the shaping phase was subdivided in several electro-thermal and mechanical parts. After each mechanical analysis the mesh was updated for the following thermal calculation. The process was aborted if the temperature within the necking zone exceeded the melting temperature of the wire material.

The whole process described above is summarized in a chart in Figure 3.

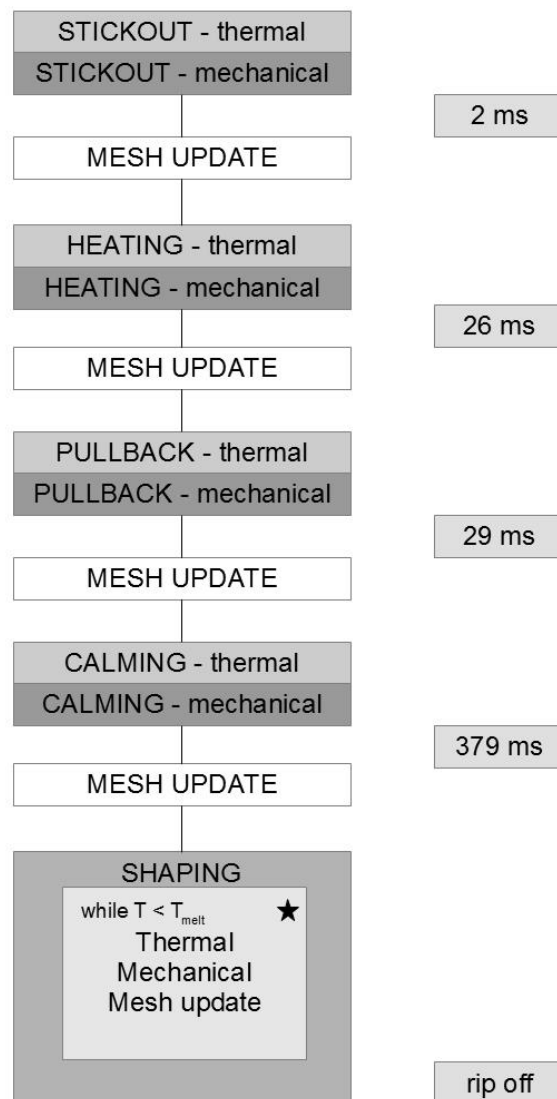


**Figure 3: Flow chart of the welding process of a single pin. The light gray boxes represent electro-thermal calculations the dark gray boxes mechanical calculations. The star in the shaping box indicates that these processes were repeated.**

### 3 Results

#### 3.1 Parameter study of $h_c$

As mentioned above, the convective heat transfer coefficient can be assumed to be different in the region of the pin plate interface than in the other areas of the system. In order to investigate the influence of different values for  $h_c$  in the interfacial area we conducted several calculations with values for  $h_c$  ranging from 80 to 200  $\text{Wm}^{-2}\text{K}^{-1}$ , all other parameters were kept constant. In Figure 4 the temperature distribution after the calming phase is depicted for different  $h_c$ . Higher values of  $h_c$  in the region of the pin socket enhances the heat flow out of the wire and thus causes the zone of maximum temperature to migrate higher upwards the wire. However the absolute value of the maximum temperature gets lower with rising  $h_c$ .

The vertical position of the hottest zone eventually defines the height of the pin because the electrical resistance is largest there.

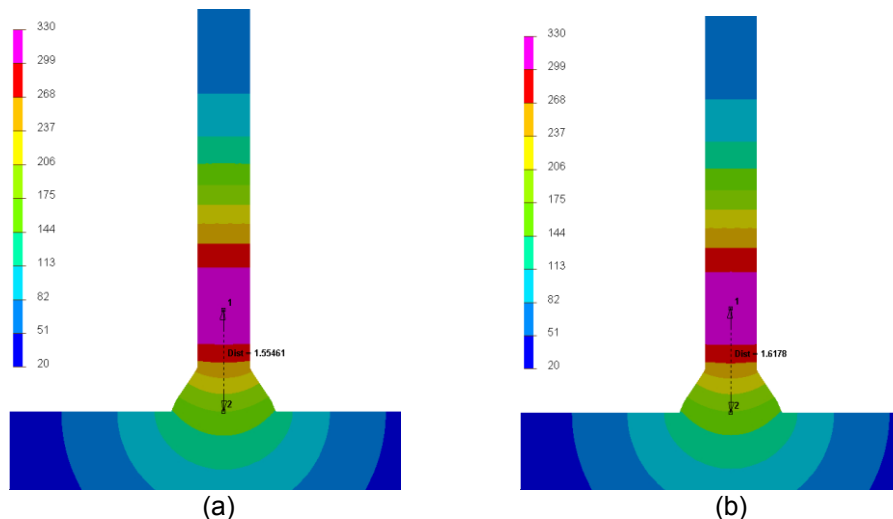


**Figure 4: Temperature fields for different values of  $h_c$ . The plotted distance markers indicate the distance of the zone with maximum temperature to surface of the base material. (a)  $h_c = 80 \text{ Wm}^{-2}\text{K}^{-1}$ , (b)  $h_c = 200 \text{ Wm}^{-2}\text{K}^{-1}$**

#### 3.2 Simulation of the weld pool

One of the major goals of this work was to mimic the heat input on a pin during its welding process. In Section 2.1 the applied heat source as well as the used boundary conditions are presented. In the case of stainless steel pins an arc voltage of  $U = 18 \text{ V}$  and a current of  $I = 35 \text{ A}$  was employed; the efficiency  $\eta$  was set to 82.5%. The quantities  $U$  and  $V$  were given by the experimental welding program, the efficiency was taken from literature (see[5]).

The parameters  $x_0$ ,  $y_0$  and  $f$  in Equation (1) are auxiliary parameters in order to describe the effects of the very complex processes occurring in a weld pool, e.g. fluid dynamic effects. Therefore, these parameters need to be tuned in order to make the simulated weld pool match experimental samples. Since the materials used in this work do not show metallurgical phase transformations only the molten zone in the polished cross section of a real pin and the results of the FE simulation was compared. Figure 4 shows a comparison of the simulation and experiment, the engaged parameters are listed in Table 3. The procedure for finding the parameters  $x_0$ ,  $y_0$  and  $f$  was based on a systematic optimization, i.e. the adjustment of simulation and experiment was done visually and the values of the parameters were changed manually.

**Table 3: Geometric parameters used in the Goldak heat source (compare Equation (1))**

$x_{pin}$ [mm]	$y_{pin}$ [mm]	$f_{pin}$	$x_{plate}$ [mm]	$y_{plate}$ [mm]	$f_{plate}$
0.85	0.3	0.78	0.97	0.04	0.22

The simulated weld pool appears to coincide quite well with the polished cross section of a real pin. However, the penetration into the plate is a little underestimated by the simulation while the molten area in the pin is slightly too low. Further improvements may be achieved by a systematical tuning of the geometry parameters of the heat source, e.g. by using neuronal networks [6].

At this point should be mentioned, that for all further analyses the convective heat transfer coefficient in the area of the pin socket was set to  $h_c = 10000 \text{ Wm}^{-2}\text{K}^{-1}$ . It turned out that using this value for  $h_c$  at the pin socket yields good results as far as the shape of the molten area is concerned as shown in Figure 5.

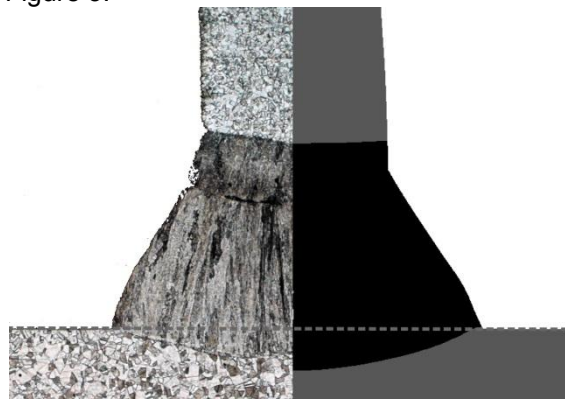


**Figure 5: Comparison of the molten zone in the simulation (left) and experiment (right) of stainless steel pins.**

In Figure 6 the temperature over time underneath the pin inside the plate is depicted and compared to measurements using thermo elements placed in a drill-hole at the lower surface of the plate. The thermo couples were attached to the plate using conductive paste (Type 'Arctic Silver' [7]). These measurements were conducted by Fronius International. The peak temperature of the measurement and the FE calculations agree pretty well, on the other hand the rate of cooling is significantly higher in the simulation than in the experiment. This results from the fact that thermal grease has a lower thermal conductivity than stainless steel. For the comparison with the experiment just the temperature of the nodes located in the same position as the thermo element was taken into account.

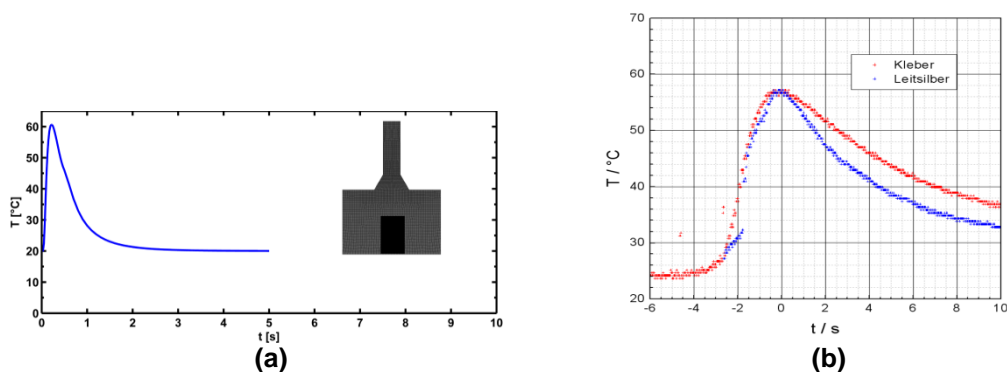


**Figure 6: Comparison between simulation (Picture (a)) and experiment (Picture (b)) of the temperature measurement. The temperature curve in Figure (a) was obtained by averaging over the nodes within the marked area.**

### 3.3 Shaping

Applying a current after a cooling time of 350 ms increases the wire's temperature at its hottest zone due to reduced electrical conductivity with increasing temperatures. Furthermore, the filler material narrows at the hottest zone due to reduced yield strength at elevated temperatures when pulling the wire upwards, leading to a reduced cross section in the zone of maximum temperature. As a consequence the filler material will heat-up at the most necked location due to Ohmic heating when a current is applied. This means that mechanical and geometrical changes have an influence on thermal electrical properties and vice versa.

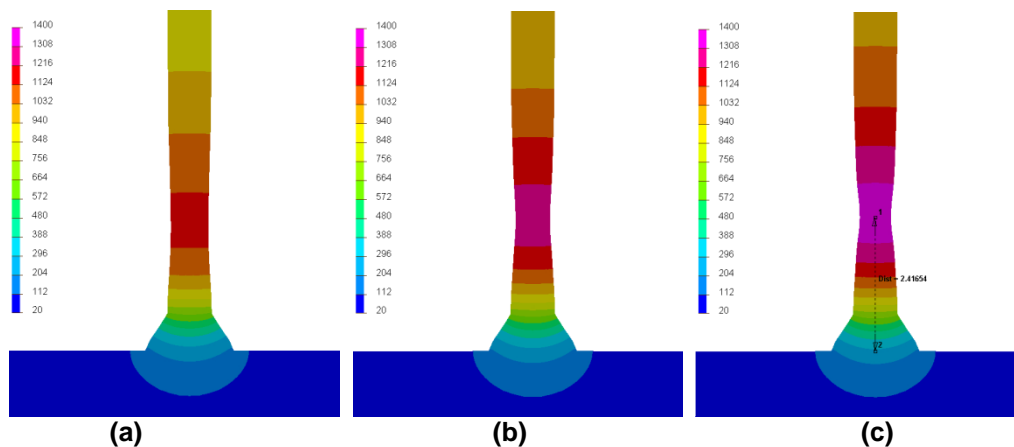


**Figure 7: Temperature distributions during the shaping phase of an electro-thermal mechanical coupled simulation. Picture (a) at 450 ms, Picture (b) at 455 ms and Picture (c) at 459 ms when the wire breaks.**

Figure 7 shows the temperature distribution during the shaping stage at several time steps before the wire rips off. One can see that the temperature reaches its maximum right in the necking zone and thus causes the wire to rip at a very defined height. Another feature in Figure 7 is that when approaching the breaking of the wire the hottest zone gets more localized, i.e. the vertical expansion of the area of maximum temperature decreases.

## 4 Conclusion

The Goldak heat source was applied successfully in order to describe the heat input during the welding process of a pin. The shape of the weld pool predicted in the simulation matches the experimental results quite well.

Further, the coupling of electro-thermal and mechanical calculations was performed for modeling the shaping of a cylindrical pin.

## 5 Outlook

As mentioned in the previous section the geometry parameters ( $x_0$ ,  $y_0$ ,  $f$ ) for the Goldak heat source were determined empirically by trial and error. A more systematic way would be using neuronal networks being a widely used tool for such tasks as described in [8].

Furthermore, the correlation of the timespan between applying the current and pulling the wire upwards at the beginning of the shaping phase, and the eventual height of the pin will be subject to further investigations.

The energy loss due to convective heat transfer is assumed to be higher in the region of the pin socket due to vortices of the shielding gas. In order to determine an actual value for  $h_c$  fluid dynamic calculations are necessary.

## 6 Acknowledgements

This work was funded by the project JOIN4+. The K-Project Network of Excellence for Joining Technologies JOIN4+ is fostered in the frame of COMET - Competence Centers for Excellent Technologies by BMVIT, BMWFJ, FFG, Land Oberösterreich, Land Steiermark, SFG and ZIT. The program COMET is handled by FFG.

## 7 References

Anca, A. and Cardona, A. and Risso, J. and Fachinotti, V.D. (2010): "Finite element modeling of welding processes," *Appl.Math.Model.*, vol. 35, no. 2, 2, pp. 688-707.

Arctic Silver Thermal Adhesive: [http://www.arcticsilver.com/arctic\\_silver\\_thermal\\_adhesive.htm](http://www.arcticsilver.com/arctic_silver_thermal_adhesive.htm)

Bhadেশia, H. (1999): "Neural networks in materials science," *ISIJ Int*, vol. 39, no. 10, pp. 966-979.

Goldak, J. and Chakravarti, A. and Bibby, M. (2011): "A new finite element model for welding heat sources," *Metallurgical and Materials Transactions B*, vol. 15, no. 2, pp. 299-305.

Incropera, F.P. and Dewitt, D.B. and Bergman, T. L. and Lavine, A. (2007): "Fundamentals of heat and mass transfer", *John Wiley, Hoboken, NJ*

Schnubel, D. and Möller, M. and Huber, N. (2011): "Boundary condition identification for structural welding simulation via artificial neural networks," *IWOTE 2011*, pp. 1-14.

Ucsnik, S. and Scheerer, M. and Zaremba, S. and Pahr, D.H. (2010): "Experimental investigation of a novel hybrid metal-composite joining technology," *Composites Part A: Applied Science and Manufacturing*, vol. 41, no. 3, pp. 369-374.

Wang, Y. and Shi, Q. and Tsai, H.L. (2001): "Modeling of the effects of surface-active elements on flow patterns and weld penetration," *Metallurgical and Materials Transactions B*, vol. 32, no. 1, pp. 145-161.